SFN Gain Simulations in Non-Interfered and Interfered SFN Network

Jyrki T.J. Penttinen
Member, IEEE
jyrki.penttinen@nsn.com

Abstract

The DVB-H (Digital Video Broadcasting, Hand-held) coverage area depends mainly on the area type, i.e. on the radio path attenuation, as well as on the transmitter power level, antenna height and radio parameters. The latter set has effect also on the audio / video capacity. In the detailed network planning, not only the coverage itself is important but the quality of service level should be dimensioned accordingly.

This paper describes the SFN gain related items as a part of the detailed radio DVB-H network planning. The emphasis is put to the effect of DVB-H parameter settings on the error levels caused by the over-sized Single Frequency Network (SFN) area. In this case, part of the transmitting sites converts to interfering sources if the safety distance margin of the radio path is exceeded. A respective method is presented for the estimation of the SFN interference levels. The functionality of the method was tested by programming a simulator and analyzing the variations of carrier per interference distribution. The results show that the theoretical SFN limits can be exceeded e.g. by selecting the antenna height in optimal way and accepting certain increase of the error level that is called SFN error rate (SER) in this paper. Furthermore, by selecting the relevant parameters in correct way, the balance between SFN gain and SER can be planned in controlled way.

Index Terms—*Mobile broadcast, single frequency network, radio planning, performance evaluation.*

1. Introduction

The DVB-H is an extended version of the terrestrial television system, DVB-T. Both are defined in the ETSI standards along with the satellite and cable versions of the DVB.

The mobile version of DVB suits especially for the moving environment as it has been optimized for the fast variations of the field strength and different terminal speeds. Furthermore, DVB-H is suitable for the delivery of various audio / video channels in a single bandwidth, and the small terminal screen shows adequately the lower resolution streams compared to the full scale DVB-T.

As DVB-H is meant for the mobile environment, the respective terminals are often used on a street level for the reception. This creates a significant difference in the received power level compared to DVB-T which uses fixed and directional rooftop antenna types. Furthermore, the DVB-H terminal has normally only small, in-built panel antenna, which is challenging for the reception of the radio signals.

The DVB-H service can be designed using either Single Frequency Network (SFN) or Multi Frequency Network (MFN) mode. In the former case, the transmitters can be added within the SFN area without co-channel interferences even if the cells of the same frequency overlap. In fact, the multi-propagated SFN signals increases the performance of the network by producing SFN gain.

Especially in the Single Frequency Network, the coverage planning is straightforward as long as the maximum distance of the sites does not exceed the allowed value defined by the guard interval (GI). The guard interval takes care of the safe reception of the multi-path propagated signals originated from various sites or due to the reflected radio waves. If the GI and FFT dependent geographical SFN boundary is ex-ceeded, part of the sites starts to act as interferers instead of providing useful carrier.

The maximum size of the non-interfered Single Frequency Network of DVB-H depends on the guard interval and FFT mode. The distance limitation between the extreme transmitter sites is thus possible to calculate in ideal conditions. Nevertheless, there might be need to extend the theoretical SFN areas e.g. due to the lack of frequencies.

Sites that are located within the SFN area minimises the effect of the inter-symbol-interferences as the guard interval protects the OFDM signals of DVB-H,

although in some cases, sufficiently strong multipath signals reflected from distant objects might cause interferences in tightly dimensioned network. On the other side, if certain degradation in the quality level of the received signal is accepted, it could be justified to even extend the SFN limits.

This paper is an extension to [1] and presents first DVB-H radio network dimensioning and SFN principles. A simulation method that was developed for estimating the balance of the SFN interference level and the SFN gain, is presented next. Case studies were carried out by utilizing a set of DVB-H radio parameters. The results shows the variations in the carrier per noise and interference levels, $C / (N + I)$, in function of related radio parameters in over-sized SFN.

2. DVB-H Dimensioning

The main link budget items affecting on the dimensioning of the DVB-H network are capacity and coverage related parameters. They also have inter-dependencies so the final dimensioning requires iterative approach.

2.1. Capacity Planning

In the initial phase of the DVB-H network planning, the offered capacity of the system is dimensioned. The total capacity in certain DVB-H band – defined as 5, 6, 7, or 8 MHz – does have effect also on the size of the coverage area. The dimensioning process is thus iterative, with the aim to find a balance between the capacity, coverage and the cost of the network.

The capacity can be varied by tuning the modulation, guard interval, code rate and channel bandwidth. As an example, the parameter set of QPSK, GI ¼, code rate ½ and channel bandwidth 8 MHz provides a total capacity of 4.98 Mb/s, which can be divided between one or more electronic service guides (ESG) and various audio / video sub-channels with typically around 200-500 kb/s bit stream dedicated for each. The capacity does not depend on the number of carriers (FFT mode) but the selected FFT affects though on the Doppler shift tolerance. As a comparison, the parameter set of 16-QAM, GI 1/32, code rate 7/8 and channel bandwidth of 8 MHz provides a total capacity of 21.1 Mb/s. It should be noted, though, that the latter parameter set is not practical due to the clearly increased C/N requirement. The relation between the radio parameter values, Doppler shift tolerance and capacity can be investigated more thoroughly in [2].

2.2. Coverage Planning

When the coverage criteria are known, the cell radius can be estimated by applying the link budget calculation. The generic principle of the DVB-H link budget can be seen in Table 1. The calculation shows an example of the transmitter output power level of 2,400 W with the quality value of 90% for the area location, though assuming that the SFN gain does not exist. According to the link budget, the outdoor reception of this specific case yields a successful reception when the radio path loss is equal or less than 140.3 dB.

Table 1. An example of DVB-H link budget.

Parameters	*Symbol*	*Value*
General parameters		
Frequency	f	680.0 MHz
Noise floor for 6 MHz BW	P_n	-106.4 dBm
RX noise figure	F	5.2 dB
Transmitter (TX)		
Transmitter output power	P_{TX}	2,400.0 W
Transmitter output power	P_{TX}	63.8 dBm
Cable and connector loss	L_{cc}	3.0 dB
Power splitter loss	L_{ps}	3.0 dB
Antenna gain	G_{TX}	13.1 dBi
Antenna gain	G_{TX}	11.0 dBd
Eff. Isotropic Radiating Power	$EIRP$	70.9 dBm
Eff. Isotropic Radiating Power	$EIRP$	12,308.7 W
Eff. Radiating Power	ERP	68.8 dBm
Eff. Radiating Power	ERP	7,502.6 W
Receiver (RX)		
Min. C/N for the used mode	$(C/N)_{min}$	17.5 dB
Sensitivity	P_{RXmin}	-83.7 dBm
Antenna gain, isotropic ref.	G_{RX}	-7.3 dBi
Antenna gain, ½ wave dipole	G_{RX}	-5.2 dBd
Isotropic power	P_i	-76.4 dBm
Loc. variation.	L_{iv}	7.0 dB
Building loss	L_b	14.0 dB
GSM filter loss	L_{GSM}	0.0 dB
Min. req. received power outd.	$P_{min(out)}$	-69.4 dBm
Min. req. received power ind.	$P_{min(in)}$	-55.4 dBm
Min. req. field strength outd.	$E_{min(out)}$	64.5 dBµV/m
Min. req. field strength ind.	$E_{min(in)}$	78.5 dBµV/m
Maximum path loss, outdoors	$L_{pl(out)}$	140.3 dB
Maximum path loss, indoors	$L_{pl(in)}$	126.3 dB

The Okumura-Hata model [3] can be applied in order to obtain the estimation for the cell radius (unit in kilometres) e.g. in large city type:

$$L(dB) = 69.55 + 26.16\lg(f) - 13.82\lg(h_{BS}) - a(h_{MS})_{type} + [44.9 - 6.55\lg(h_{BS})]\lg(d) \quad (1)$$

For $f \geq 400$ MHz, the area type factor is:

$$a(h_{MS})_{LC} = 3.2[\lg(11.75h_{MS})]^2 - 4.97 \quad (2)$$

$$d = 10^{\left(\frac{L(dB)-[69.55+26.16\lg(f)-13.82\lg(h_{BS})-a(h_{MS})_i]}{44.9-6.55\lg(h_{BS})}\right)} \quad (3)$$

Figure 1 presents the estimated cell range of the example that is calculated with the large city model and by varying the transmitter antenna height and power level. As can be noted, the antenna height has major impact on the cell radius compared to the transmitter power level.

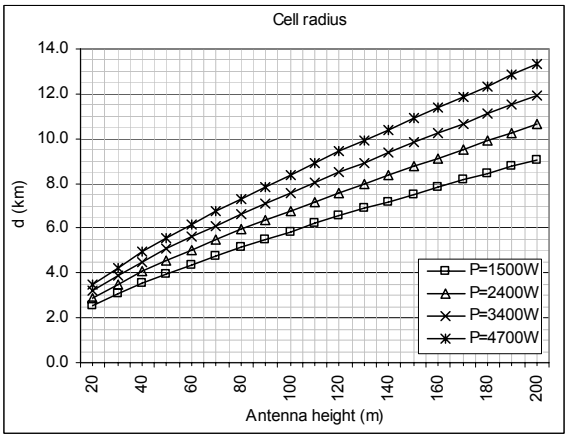

Figure 1. The cell range calculated with the Okumura-Hata model for the large city, varying the transmitter power levels.

In the SFN related reference material, different values for the SFN gain is proposed to be added to the DVB-H link budget, typically from 0 to 3 dB. As an example, [4] mentions that due to the large standard variation of the combined signal reception in environment with multi-path propagation, no SFN gain is recommended for the planning criteria. In the same document, a SFN gain of around 1.5 dB was obtained for the 2 transmitter case by carrying out field measurements. A 3-transmitter field measurement case can be found in [5], which shows that about 2 dB SFN gain was achieved. For the large amount of sites, no practical field results can be found due to the complexity of the test setup.

Nevertheless, the possible SFN gain of, e.g., 2 dB would have around same effect on the coverage area growth as changing the 1500 W transmitter to 2400 W power level category, i.e. there can be an important cost effect in selected areas of the DVB-H network depending on the functionality of the SFN gain.

3. Theory of the SFN Limits

The DVB-H radio transmission is based on the OFDM (Orthogonal Frequency Division Multiplexing). The idea of the technique is to create various separate data streams that are delivered in sub-bands. The error correction is thus efficient as the sufficiently high-quality sub-bands are used for the processing of the received data, depending on the level of the correction schemes used in the transmission.

In order to work, the system needs to minimize the interference levels between the sub-bands. The sub-band signals should thus be orthogonal. In order to comply with this requirement, the carrier frequencies are selected in such way that the spacing between the adjacent channels is the inverse of symbol duration.

According to [2], the GI and the FFT mode determinate the maximum delay that the mobile can handle for receiving correctly the multi-path components of the signals. The Table 2 summarises the maximum allowed delays and respective distances. The maximum allowed distance per parameter setting has been calculated assuming the radio signal propagates with the speed of light.

Table 2. The guard interval lengths and respective safety distances.

GI	*FFT = 2K*	*FFT = 4K*	*FFT = 8K*
1/4	56 µs / 16.8 km	112 µs / 33.6 km	224 µs / 67 km
1/8	28 µs / 8.4 km	56 µs / 16.8 km	112 µs / 33.6 km
1/16	14 µs / 4.2 km	28 µs / 8.4 km	56 µs / 16.8 km
1/32	7 µs / 2.1 km	14 µs / 4.2 km	28 µs / 8.4 km

As long as the distance between the extreme transmitter sites is less than the safety margin dictates, the difference of the delays between the signals originated from different sites never exceeds the allowed value unless there is a strong multipath propagated signal present.

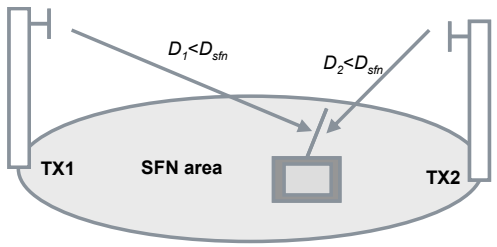

Figure 2. If all the sites of certain frequency band are located inside the SFN area with the distance between the extreme sites less than D_{sfn}, no inter-symbol interferences are produced.

On the other hand, when the terminal drifts outside of the original SFN area and receives sufficiently strong signals from the original SFN, no problems arises either in this case as it can be shown that the difference of the signal delays from the respective SFN sites are always within the safety limits.

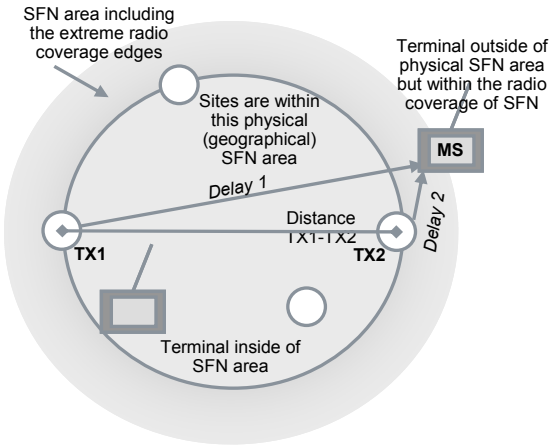

Figure 3. The GI applies also outside the physical SFN cell area where the signal level originated form the SFN is sufficiently high.

The situation changes if the inter-site distance exceeds the allowed theoretical value. As an example, GI of 1/4 and 8K mode provide 224 µs margin for the safe propagation delay. Assuming the signal propagates with the speed of light, the SFN size limit is 300,000 km/s · 224 µs yielding about 67 km of maximum distance between the sites. If any geographical combination of the site locations using the same frequency exceeds this maximum allowed distance, they start producing interference in those spots where the difference of the arriving signals is higher than 224 µs.

If the level of interference is greater than the noise floor, and the minimum C/N value that the respective mode required in non-interfered situation is not any more obtained, the signal in that specific spot is interfered and the reception suffers from the frame errors that disturb the fluent following of the contents. In order to achieve correct reception, the additional interference increases the required received power level of the carrier to $C/N \rightarrow C / (N + I)$.

Figure 4 shows that if the D_{eff}, i.e. the difference between the signals arriving from the sites, is more than the allowed safety distance in over-sized SFN, the site acts as an interferer. Whilst the carrier per interference and noise level from the TX_2 complies with the minimum requirement for the C/N, the transmission is still useful.

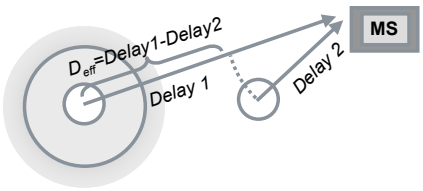

Figure 4. When the mobile station is receiving signals from the over-sized SFN-network, the sum of the interfering signals might destroy the reception if their level is sufficiently high compared to the sum of the useful carrier levels.

Even if the $C / (N + I)$ level gets lower when the terminal moves from one site to another, the situation is not necessarily critical as the effective distance D_{eff} of the signals might be within the SFN limits e.g. in the middle of two sites, although their distance from each others would be greater than the maximum allowed. In other words, the otherwise interfering site might not be considered as interference in the respective spot but it might give SFN gain by producing additional carrier C_2. This phenomenon can be observed in practice as the SFN interferences tends to accumulate primarily in the outer boundaries of the network.

Figure 5 shows the principle of the relative interference which increases especially when the terminal moves away from the centre of the SFN network.

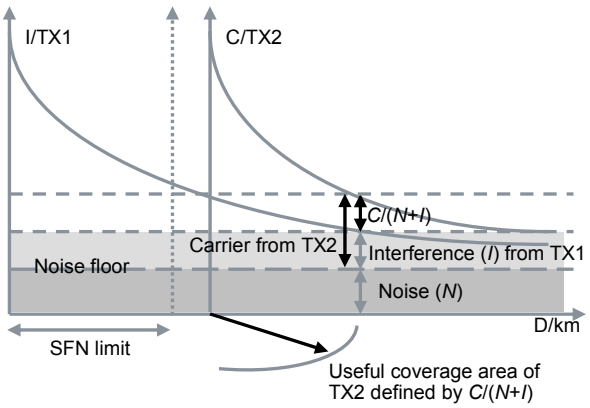

Figure 5. The principle of interference when the location of transmitter TX_1 is out of the SFN limit.

When moving outside of the network, the relative difference between the carrier and interfering signal gets smaller and it is thus inevitable that the $C / (N + I)$ will not be sufficient any more at some point for the correct reception of the carrier, although the C/N level without the presence of interfering signal would still be sufficiently high. The essential question is thus, where the critical points are found with lower $C / (N + I)$

value than the original requirement for *C*/*N* is, and where the interference thus converts active, i.e. when D_{eff} is longer than the safety margin.

As an example, the distance of two sites could be 70 km, which is more than D_{sfn} with any of the radio parameter combination of DVB-H. For the parameter set of FFT 8k and GI 1/8, the safety distance for D_{sfn} is about 34 km, which is clearly less than the distance of these sites. Let's define the radiating power (EIRP) for each site to +60 dBm. We can now observe the received power level of the sites in the theoretical open area by applying the free space loss, *f* representing the frequency (MHz) and *d* the distance (km):

$$L = 20\log f + 20\log d + 32.44 \quad (4)$$

Figure 6 shows the carrier (or interference) from TX_1 located in 0 km and carrier (or interference) from TX_2 located in 70 km, when the parameter set allows D_{sfn} of 34 km. The interference is included in those spots where the D_{eff} is higher than D_{sfn}. If the D_{eff} is shorter than D_{sfn}, the respective received useful power level is shown taking into account the SFN gain of these two sites by summing the absolute values of the power levels:

$$C_{tot} = \sqrt{C_1^2 + C_2^2} \quad (5)$$

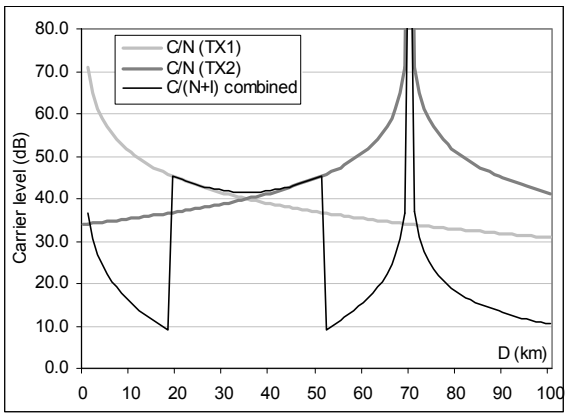

Figure 6. The combined *C*/(*N*+*I*) along the route from 0 to 100 km, taking into account the SFN-gain when the interference is not present.

As Figure 6 shows, the TX_1 is acting as a carrier and TX_2 as interferer from 0 km (TX_1 location) to 18 km, because the $D_{eff} > D_{sfn}$. Nevertheless, the carrier of TX_1 is dominating within this area in order to provide sufficiently high $C / (N + I)$ for the successful reception for the QPSK, CR 1/2 and MPE-FEC 1/2 as it requires 8.5 dB. The segment of 18 km to 52 km is clear from the interferences as all the $D_{eff} < D_{sfn}$, and in addition, the receiver gets SFN gain from the combined carriers of TX_1 and TX_2. The TX_1 starts to act as an interferer from 52 km to 100 km (or, until the *C*/*N* limit of the used mode). Nevertheless, the interference of TX_1 is already so attenuated such a far away from its origin that the $C / (N + I)$ is high enough for the successful reception from TX_2 of above mentioned QPSK still within the area of 80 – 100km. With any other parameter settings, the SFN interference level is high enough to affect on the successful reception in these breaking points where the D_{eff} makes the signal act as interferer instead of carrier.

As can be seen from this example, the interference level takes place when the terminal moves towards the boundaries or boundary sites of the network. As a result, the boundary site's coverage area gets smaller, and depending on the parameter setting, there will be interferences between the sites.

The required *C*/*N* for some of the most commonly used parameter setting can be seen in Table 3 [2]. The terminal antenna gain (loss) is taken into account in the presented values. The Table present the expected *C*/*N* values in Mobile TU-channel (typical urban) for the "possible" reference receiver.

Table 3. The minimum *C*/*N* (dB) for the selected parameter settings.

Parameters	*C/N*
QPSK, CR 1/2, MPE-FEC 1/2	8.5
QPSK, CR 1/2, MPE-FEC 2/3	11.5
16-QAM, CR 1/2, MPE-FEC 1/2	14.5
16-QAM, CR 1/2, MPE-FEC 2/3	17.5

The FFT size has impact on the maximum velocity of the terminal, and the GI affects on both the maximum velocity as well as on the capacity of the radio interface. In fact, in these simulations, if only the requirement for the level of carrier is considered without the need to take into account the maximum functional velocity of the terminal or the radio channel capacity, the following parameter combinations results the same *C*/*N* and $C / (N + I)$ performance due to their same requirement for the safety distances:

- FFT 8K, GI 1/4: only one set
- FFT 8K, GI 1/8: same as FFT 4K, GI 1/4
- FFT 8K, GI 1/16: same as FFT 4K, GI 1/8 and FFT 2K, GI 1/4
- FFT 8K, GI 1/32: same as FFT 4K, GI 1/16 and FFT 2K, GI 1/8
- FFT 4K, GI 1/32: same as FFT 2K, GI 1/16
- FFT 2K, GI 1/32: only one set

4. Methodology for the SFN simulations: first variation (unlimited SFN network)

4.1. General

In order to estimate the error level of various sites that is caused by extending the theoretical geometrical limits of SFN network, a simulation can be carried out as presented in [6]. For the simulation, the investigated variables can be e.g. the antenna height and power level of the transmitter, in addition to the GI and FFT mode that defines the SFN limits.

The setup for the simulation consists of radio propagation type and geometrical area where the cells are located. The most logical way is to dimension the network according to the radio interface parameters, i.e. the cell radius should be dimensioned according to the minimum *C*/*N* requirement.

For this, a link budget calculator is included to the initial part of the simulator. It estimates the radius for both useful carriers as well as for the interfering signals, noise level being the reference.

Depending on the site definitions, there might be need to apply other propagation models as the basic Okumura-Hata [3] is valid for the maximum cell radius of 20 km and antenna heights up to 200 m. One of the suitable models for the large cells is ITU-R P.1546 [7] which is based on the interpolation of the pre-calculated curves.

When estimating the total carrier per interference levels, both total level of the carriers and interferences can be calculated separately by the following formulas, using the respective absolute power levels (W) for the *C* and *I* components:

$$C_{tot} = \sqrt{C_1^2 + C_2^2 + ... + C_n^2} \quad (6)$$

$$I_{tot} = \sqrt{I_1^2 + I_2^2 + ... + I_n^2} \quad (7)$$

In each simulation round, the site with the highest field strength is identified. In case of uniform network and equal site configurations, the site with lowest propagation loss corresponds to the nearest cell TX_1 which is selected as a reference. Once the nearest cell is identified, the task is to investigate the propagation delays of signals between the nearest and each one of the other sites, and calculate if the difference of arriving signals D_{eff} is greater or lower than the SFN limit D_{sfn}. In general, if the difference of the signal arrival times of TX_1 and TX_n is greater than GI defines, the TX_n is producing interfering signal (if the signal is above the noise floor), and otherwise it is adding the level of total carrier energy (if the signal level is above the minimum requirement for carrier).

In order to obtain the level of *C* and *I* in certain area type, the path loss can be estimated with Okumura-Hata radio propagation model or ITU-R P.1546.

The total path loss can be calculated by applying the following formula:

$$L_{tot} = L_{pathloss} + L_{norm} + L_{other} \quad (8)$$

L_{norm} represents the fading loss caused by the long-term variations, and other losses may include e.g. the fast fading as well as antenna losses.

For the long-term fading, a normal distribution is commonly used in order for modelling the variations of the signal level. The PDF of the long-term fading is the following [8]:

$$PDF(L_{norm}) = \frac{1}{\sqrt{2\pi}\sigma} \exp\left[\frac{-(x-\bar{x})^2}{2\sigma^2}\right] \quad (9)$$

The term x represents the loss value, and $\bar{x}$ is the average loss (0 in this case). In the snap-shot based simulations, the L_{norm} is calculated for each arriving signal individually as the different events does not have correlation. The respective PDF and CDF are obtained by creating a probability table for normal distributions. Figure 7 shows an example of the PDF and CDF of normal distributed loss variations when the mean value is 0 and standard deviation is 5.5 dB.

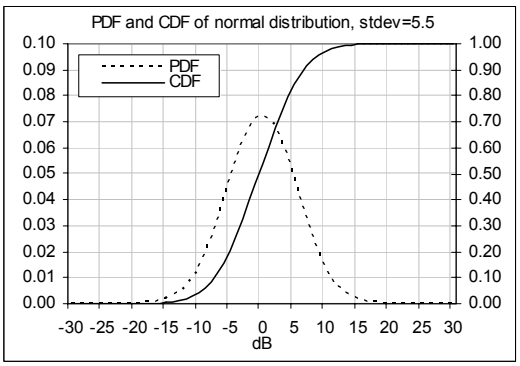

Figure 7. PDF and CDF of the normal distribution representing the variations of long-term loss when the standard deviation is set to 5.5 dB.

The fast (Rayleigh) fading is present in those environments where multi-path radio signals occurs, e.g., on the street level of cities. It can be presented with the following PDF:

$$L_{\log norm} = \frac{x}{\delta^2} e^{-(\frac{x^2}{2\delta^2})} \quad (10)$$

Figure 8 shows the PDF and CDF of the fast fading representing the variations of short-term loss when the standard deviation is set to 5.5 dB.

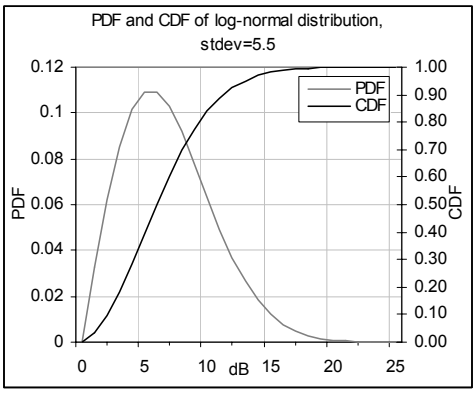

Figure 8. PDF and CDF of the log-normal distribution for fast fading.

4.2. Simulator

A block diagram of the presented SFN interference simulator is shown in Figure 9. The simulator was programmed with a standard Pascal code. It produces the results to text files, containing the *C*/*N*, *I*/*N* and *C* / (*N* + *I*) values showing the distribution in scale of -50...+50 dB and with 0.1 dB resolution, using integer type table indexes of -500 to +500 that represents the occurred cumulative values. Also the terminal coordinates and respective *C*/*N*, *I*/*N* and *C* / (*N* + *I*) for all the simulation rounds is produced. If the value occurs outside the scale, it is added to the extreme dB categories in order to form the CDF correctly.

A total of 60,000 simulation rounds per each case were carried out. It corresponds to an average of 60,000 / (50 dB · 10) = 120 samples per *C*/*I* resolution, which fulfils the accuracy of the binomial distribution. Each text file was post-processed and analysed with Microsoft Excel.

The terminal was placed randomly in 100 km × 100 km area according to the uniform distribution in function of the coordinates (*x*, *y*) during each simulation round. The raster of the area was set to 10 m. Small and medium city area type was selected for the simulations. The total *C*/*I* value is calculated per simulation round by observing the individual signals of the sites.

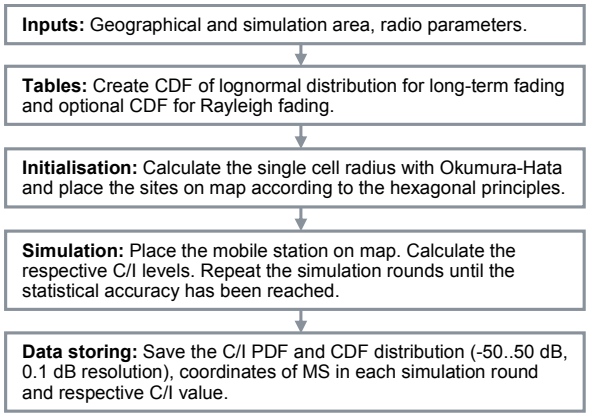

Figure 9. The simulator's block diagram.

The nearest site is selected as a reference during the respective simulation round. If the arrival time delays difference $\Delta t_2 - \Delta t_1$ is less than D_{sfn} defines, the respective signal is marked as useful carrier *C*, or otherwise it is marked as interference *I*. In the generic format, the total *C* / (*N* + *I*) can be obtained from the simulation results in the following way:

$$\frac{C}{N+I} = (C_{tot}[dB] - noisefloor[dB]) - (I_{tot}[dB] - noisefloor[dB]) \quad (11)$$

The term *N* represents the reference which is the sum of noise floor and terminal noise figure. The noise figure depends on the terminal characteristics. In the simulations, it was estimated to 5 dB as defined in [2].

The simulator calculates the expected radius of single cell in non-interfering case and fills the area with uniform cells according to the hexagonal model. This provides partial overlapping of the cells. Each simulation round provides information if that specific connection is useless, e.g. if the criteria set of 1) effective distance $D_{eff} > D_{sfn}$ in any of the cells, and 2) *C* / (*N* + *I*) < minimum *C*/*N* threshold. If both criteria are valid, and if the *C*/*N* would have been sufficiently high without the interference in that specific round, the SFN interference level is calculated.

Figure 10 shows an example of the site locations. As can be seen, the simulator calculates the optimal cell radius according to the parameter setting and locates the transmitters on map according to the hexagonal model, leaving ideal overlapping areas in the cell border areas. The size and thus the number of the cells depends on the radio parameter settings without interferences, and in each case, a result is a uniform service level in the whole investigated area. The same network setup is used throughout the

complete simulation, and changed if the radio parameters of the following simulation require so.

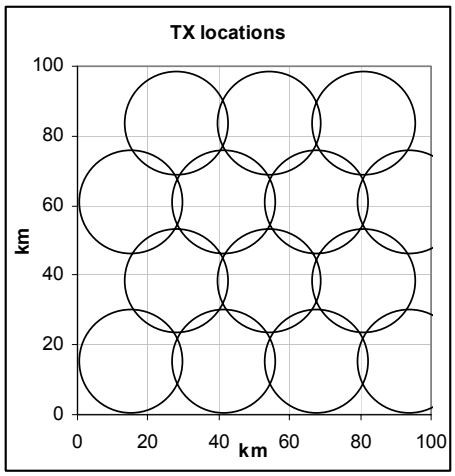

Figure 10. Example of the transmitter site locations the simulator has generated.

The behaviour of *C* and *I* can be investigated by observing the probability density functions, i.e. PDF of the results. Nevertheless, the specific values of the interference levels can be obtained by producing a CDF from the simulation results.

Figure 11 shows two examples of the simulation results in CDF format. In this specific case, the outage probability of 10% (i.e. area location probability of 90 %) yields the minimum $C / (N + I)$ of 10 dB for 8K, which complies with the original *C*/*N* requirement (8.5 dB) of this case. On the other hand, the 4K mode results about 7 dB with 10% outage, which means that the minimum quality targets can not quite be achieved any more with these settings.

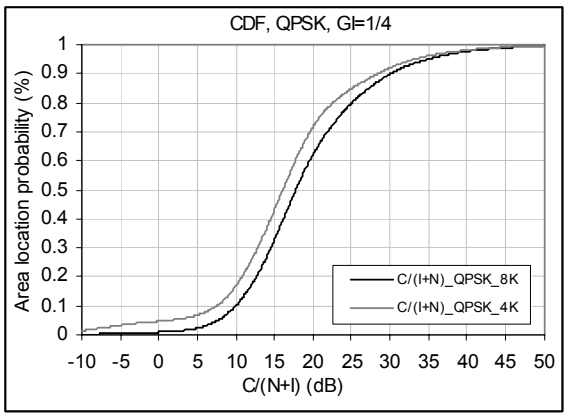

Figure 11. Example of the cumulative distribution of *C*/(*N*+*I*) for QPSK 4K and 8K modes with antenna height of 200 m and Ptx +60 dBm.

4.3. Results

By applying the principles of the DVB-H simulator, the *C*/*I* distribution was obtained according to the selected radio parameters. The variables were the modulation scheme (QPSK and 16-QAM), antenna height (20-200 m) and FFT mode (4K and 8K).

Figures 12-13 show the resulting networks that were used as a basis for the simulations. The simulator selects randomly the mobile terminal location on the map and calculates the *C*/*I* that the network produces at that specific location and moment. This procedure is repeated during 60,000 simulation rounds. One of the results after the complete simulation is the estimation for the occurred errors due to the interfering signals from the sites exceeding the safety distance (i.e. if the arrival times of the signals exceed the maximum allowed delay difference). This event can be called "SFN error rate", or SER.

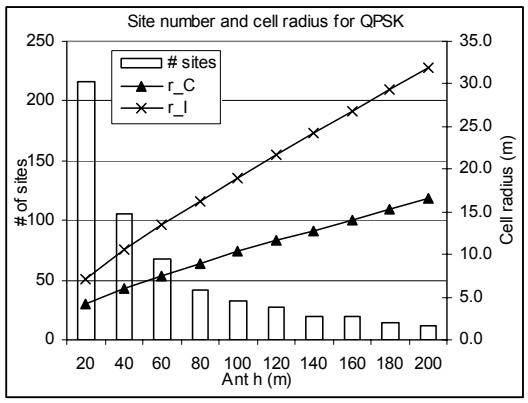

Figure 12. The network dimensions for the QPSK simulations.

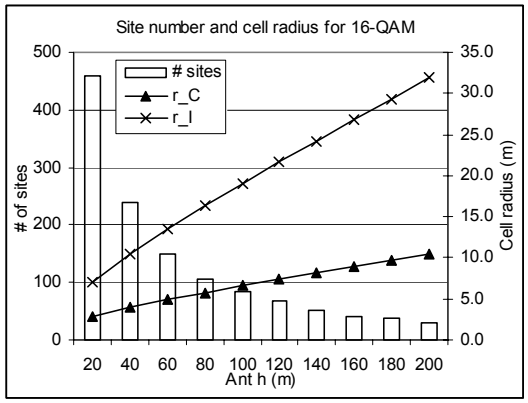

Figure 13. The network dimensions for the 16-QAM simulations.

In Figure 14, the plots indicates the locations where the results of $C / (N + I)$ corresponds 8.5 dB or less for QPSK. In this case, the interfering plots represent the relative SFN area error rate (SAER) of 0.83%, i.e. the erroneous (SAR) cases over the number of total simulation rounds as for the simulated plots.

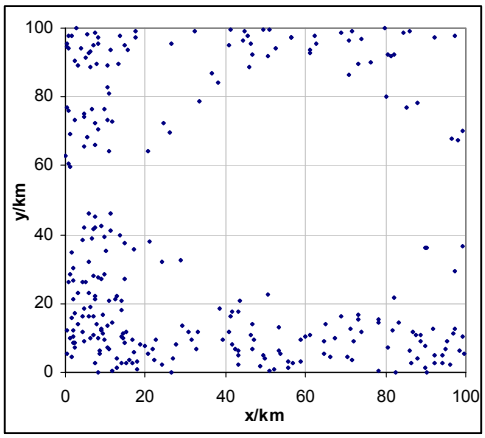

Figure 14. An example of the results in geographical format with $C/(N+I)$<8.5 dB.

It can be assumed that when the SER level is sufficiently low, the end-users will not experience remarkable reduction in the DVB-H reception due to the extended SFN limits. In this analysis, a SER level of 5% is assumed to still provide with sufficient performance as it is in align with the limits defined in [2] for frame error rate before the MPE-FEC (FER) and frame error rate after the MPE-FEC (MFER). The nature of the SER is slightly different, though, as the interferences tend to cumulate to certain locations as can be observed in Figure 14 obtained from the simulator.

According to simulations, the SFN interference level varies clearly when radio parameters are tuned. Figures 15-18 summarise the respective SFN area error analysis, the variable being the transmitter antenna height. Figures show that with the uniform radio parameters and varying the antenna height, modulation and FFT mode, the functional settings can be found regardless of the exceeding of the theoretical SFN limits.

If a 5% limit for SER is accepted, the analysis show that antenna height of about 80 m or lower produces SER of 5% or less for QPSK, 8K, with minimum $C / (N + I)$ requirement of 8.5 dB. If the mode is changed to 4K, the antenna height should be lowered to 35-40 m from ground level in order to comply with 5% SER criteria in this very case. 16-PSK produces higher capacity and smaller coverage.

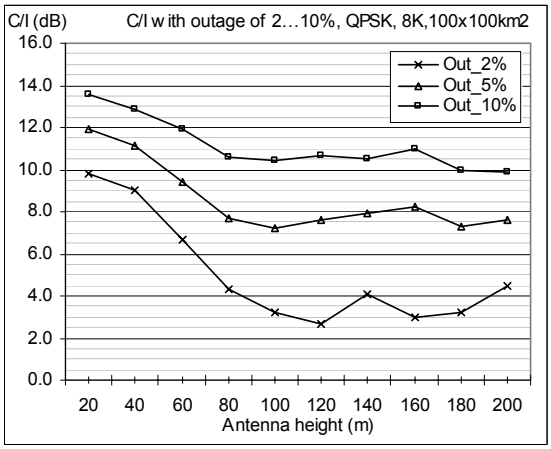

Figure 15. The summary of the case 1 (QPSK, 8K). The results show the $C/(N+I)$ with 2%, 5% and 10 % SER criteria.

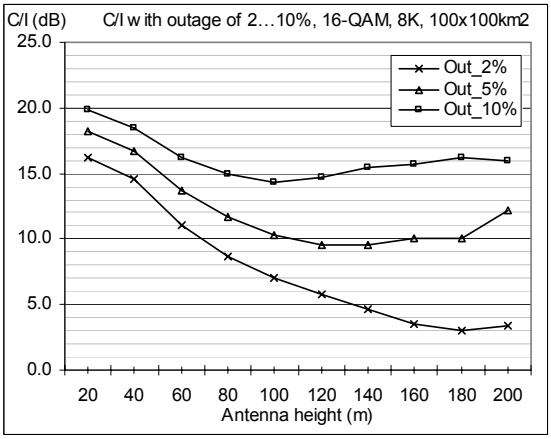

Figure 16. The summary of the case 2 (16-QAM, 8K).

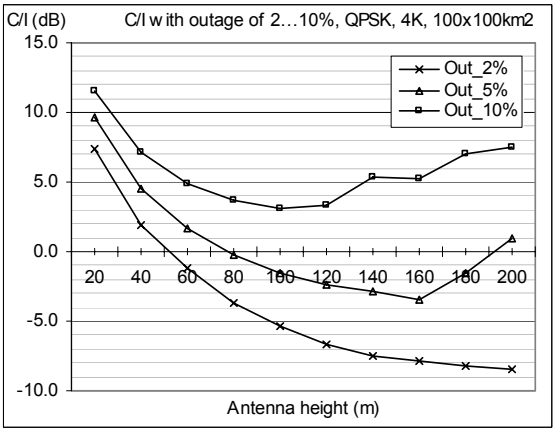

Figure 17. The summary of the case 3 (QPSK, 4K).

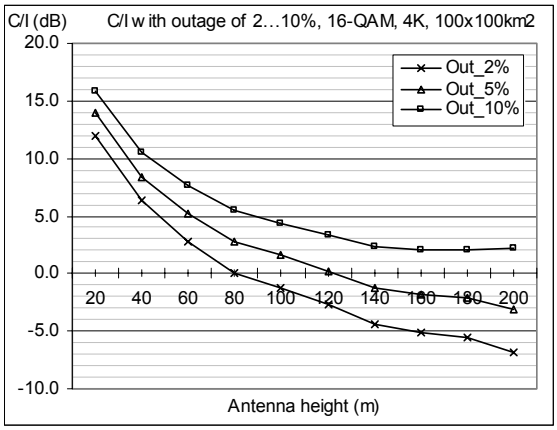

Figure 18. The summary of the case 4 (16-QAM, 4K).

The results show this clearly as the respective SER of 5% (16-QAM, 8K and minimum C / (N + I) requirement of 14.5 dB for this modulation) allows the use of antenna height of about 120 m. If the mode of this case is switched to 4K, the antenna should be lowered down to 50 m in order to still fulfil the SER 5% criteria.

The +60 dBm EIRP represents relatively low power. The higher power level raises the SER level accordingly. For the mid and high power sites the optimal setting depends thus even more on the combination of the power level and antenna height. According to these results, it is clear that the FFT mode 8K is the only reasonable option when the SER should be kept in acceptable level. Especially the QPSK modulation might not allow easily extension of SFN as the modulation provides largest coverage areas. On the other hand, when providing more capacity, 16-QAM is the most logical solution as it gives normally sufficient capacity with reasonable coverage areas. The stronger CR and MPE-FEC error correction rate decreases the coverage area but it is worth noting that the interference propagates equally also in those cases.

The general problem of the SER arises from the different loss behaviour of the useful carrier and interfering signal. Depending on the case, the interfering signal might propagate 2-3 times further away from the originating site compared to the useful carrier as can be seen from Figures 12 and 13.

In practice, the SER level can be further decreased by minimising the propagation of the interfering components. This can be done e.g. by adjusting the transmitter antenna down-tilting and using narrow vertical beam widths, producing thus the coverage area of the carrier and interference as close to each others as possible. Also the natural obstacles of the environment can be used efficiently for limiting the interferences far away outside the cell range.

Figure 19 shows the previously presented results presenting the outage percentage for the different modes having 8.5 dB C / *(N + I)* limit for QPSK and 14.5 % for 16-QAM cases in function of transmitter antenna height.

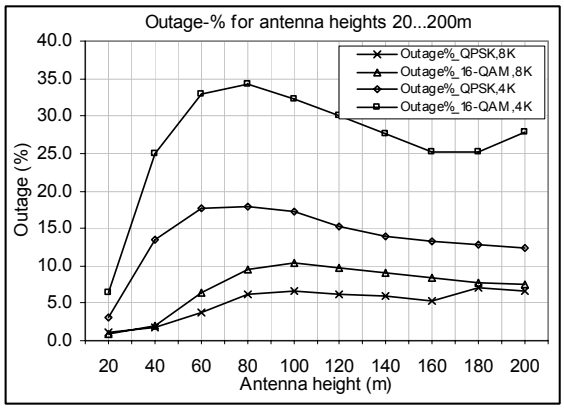

Figure 19. The summary of the cases 1-4 presenting the outage percentage in function of the transmitter antenna height.

This version of the simulator gives indication about the behaviour of the C / (N + I) in geographical area. In order to estimate the SFN gain, the individual cells could be switched on and off for the comparison of the differences in overall C / (N + I) distribution. Nevertheless, when the investigated area is filled with the cells, it normally leaves outages in the northern and eastern sides as the area cannot be filled completely as shown in Figure 10. It also produces partial cell areas, if the centre of the site fits into the area but the edge is outside. An enhanced version of the simulator was thus developed in order to investigate the SFN gain in more controlled way, i.e. instead of the fixed area size the method uses the variable reuse pattern sizes. The following Chapter 6 describes the method.

5. Methodology for the simulations: second variation (SFN network with fixed reuse patterns)

5.1. Simulator

The second version of the presented SFN performance simulator is based on the hexagonal cell layout [1]. Figure 20 presents the basic idea of the cell distribution.

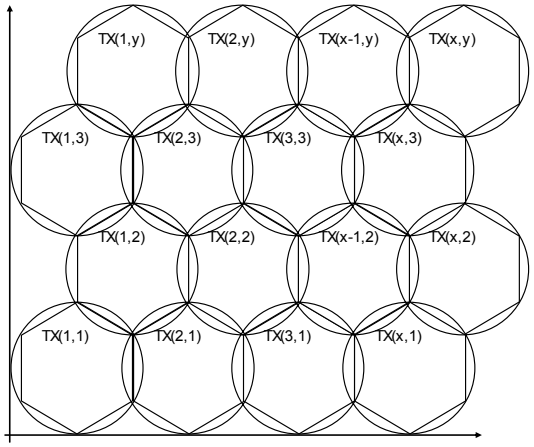

Figure 20. The active transmitter sites are selected from the 2-dimensional cell matrix with the individual numbers of the sites.

As can be seen from Figure 20, the cells are located in such way that they create ideal overlapping areas. The tightly located hexagonal cells fill completely the circle-shape cells. A uniform parameter set is used in each cell, including the transmitter power level and antenna height, yielding the same radius for each cell per simulation case.

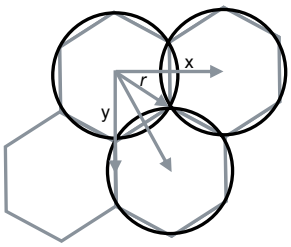

Figure 21. The *x* and *y* coordinates for the calculation of the site locations.

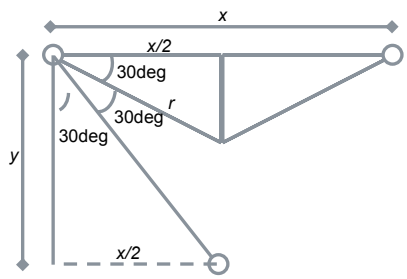

Figure 22. The geometrical characteristics of the hexagonal model used in the simulator.

As the relative location of the cells is fixed, the coordinates of each cell depends on the uniform cell size, i.e. on the radius. Taking into account the characteristics of the hexagonal model, the *x* coordinates can be obtained in the following way depending if the row for *y* coordinates is odd or even.

The distance between two sites in *x*-axis is:

$$x = 2r\cos(30°) = 2 \cdot 0.866r \tag{12}$$

The common inter-site distance in *y*-axis is:

$$y = \frac{r\cos(30°)}{\tan(30°)} = \frac{2r}{3} \tag{13}$$

For the odd rows the formula for the *x*-coordinate of the site *m* is thus the following:

$$x(m)_{odd} = r + (m-1)\cdot 1.732r \tag{14}$$

In the formula, *m* represents the number of the cell in *x*-axis. In the same manner, the formula for *x*-coordinates can be created in the following way:

$$x(m)_{even} = r + \frac{1}{2}1.732r + (m-1)\cdot 1.732r \tag{15}$$

For the *y* coordinates, the formula is the following:

$$y(n) = r + (n-1)\cdot\frac{2}{3}r \tag{16}$$

The simulations can be carried out for different cell layouts. Symmetrical reuse pattern concept was selected for the simulations presented in this paper. The most meaningful reuse pattern size *K* can be obtained with the following formula [9]:

$$K = (k-l)^2 - kl \tag{17}$$

The variables *k* and *l* are positive integers with minimum value of 0. In the simulations, the reuse pattern sizes of 1, 3, 4, 7, 9, 12, 16, 19 and 21 was used for the *C* / (*N* + *I*) distribution in order to obtain the carrier and interference distribution in both non-interfering and interfering networks (i.e. SER either exists or not depending on the size of the SFN area). In this way, the lower values of *K* provides with the non-interfering SFN network until a limit that depends on the GI and FFT size parameters.

The single cell (*K*=1) is considered as a reference in all of the cases. The fixed parameter set was the following:

- Transmitter power: 60 dBm
- Transmitter antenna height: 60 m

- Receiver antenna height: 1.5 m
- Long-term fading with normal distribution and standard deviation of 5.5 dB
- Area coverage probability in the cell edge: 70%
- Receiver noise figure: 5 dB
- Bandwidth: 8 MHz
- Frequency: 700 MHz

For the used bandwidth, the combined noise floor and noise figure yields -100.2 dBm as a reference for calculating the level of *C* and *I*. The path loss was calculated with Okumura-Hata prediction model for small and medium sized city. The 70 % area coverage probability corresponds with 10% outage probability in the single cell area.

These settings result a reference *C*/*N* of 8.5 dB for QPSK and 14.5 dB for 16-QAM. The value is the minimum acceptable *C*/*N*, or in case of interferences, *C* / (*N* + *I*) value that is needed for the successful reception of the signal.

Figures 23 and 24 present the symmetrical reuse patterns that were selected for the simulations. The grey hexagonal means that the coordinates has been taken into account calculating the order number of the sites according to the formulas 14-16, but the respective transmitter has been switched off in order to form the correct reuse pattern.

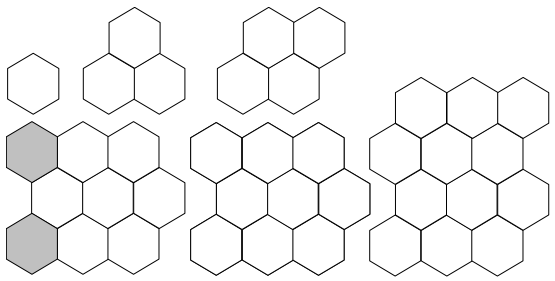

Figure 23. The reuse patterns with *K* of 1, 3, 4, 7, 9 and 12.

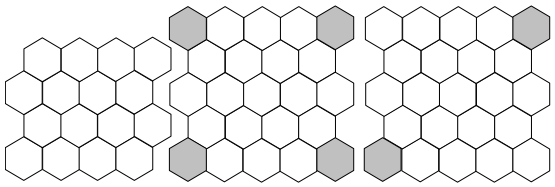

Figure 24. The reuse patterns with *K* of 16, 19 and 21.

Figure 25 shows the site locations for the QPSK and *K*=7, and Figure 26 shows an example of the *C*/*N* distribution with the parameter values of *K*=7, GI=1/4, and FFT=8K.

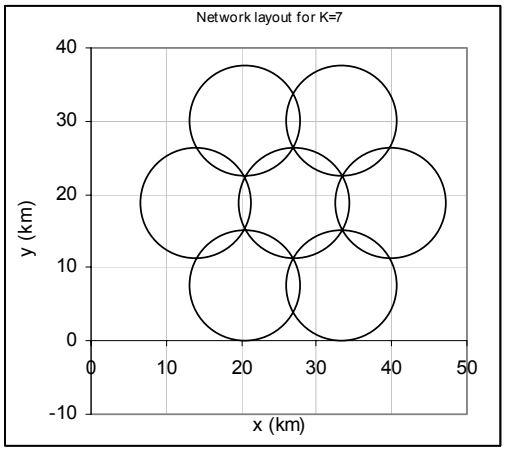

Figure 25. An example showing the layout of the QPSK network with *K*=7.

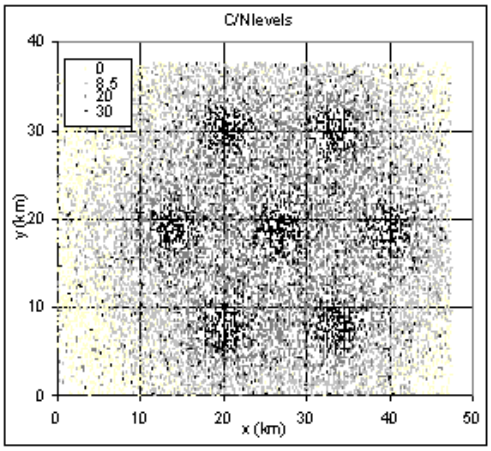

Figure 26. An example of the simulated case with QPSK and *K*=7.

According to the *C*/*I* link analysis, the case presented in Figure 26 is free of SFN interferences.

The actual simulation results for *C*/*N*, or in case of the interferences, for *C* / (*N* + *I*), is done in such way that only the terminal locations inside the calculated cell areas are taken into account. If the terminal is found outside of the network area (the circles) in some simulation round, the result is simply rejected.

Figure 27 shows the principle of the filtered simulation. As the terminal is always inside the coverage area of at least one cell, it gives the most accurate estimation of the SFN gain with different parameter values. Furthermore, the method provides a reliable means to locate the MS inside the network area according to the uniform distribution.

The network is dimensioned in such way that the area location probability is 70% in the cell edge. The

dimensioning can be made according to the characteristics of long-term fading.

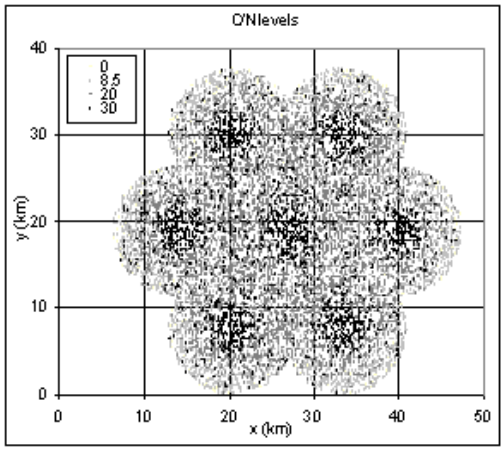

Figure 27. The filtered simulation area. This principle is used in the simulations in order to keep the network borders always constant. If the mobile station is inside the planned network area, it provides a reliable estimation of the SFN gain.

Figure 28 shows snap-shot type example of the *C*/*N* values with less than 8.5 dB, which is the limit for the respective parameter settings of QPSK cases.

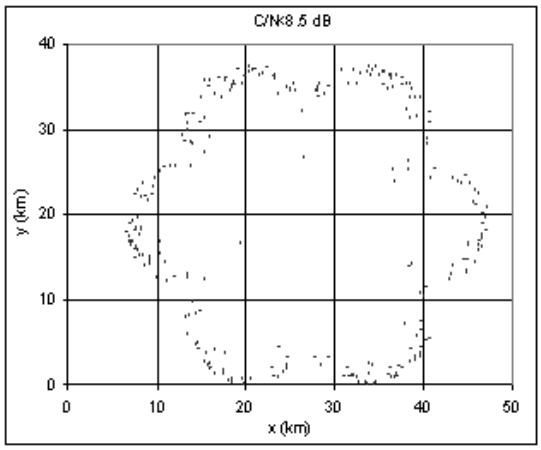

Figure 28. An example of the distribution of the simulation results that yields less than 8.5 dB for the *C*/*N*.

As a verification of the geographical interference class, a study that can be called a *C*/*I*-link analysis can be carried out. It is a method to revise all the combinations (hash) of the distances between each pair of sites (TX_1-TX_2, TX_1-TX_3, TX_2-TX_1, TX_2-TX_3 etc.) marking the link as useful (*C*) if the guard distance between the respective sites is less than the maximum allowed SFN diameter (D_{sfn}). If the link is longer, it is marked as a potential source of interference (*I*). The interference link proportion can be obtained for each case by calculating the interference links over the total links. It gives a rough idea about the "severity" of the exceeding of the SFN limit, with a value range of 0-100% (from non-interfering network up to interfered network where all the transmitters are a potential source of interference).

5.2. Results

Tables 4 and 5 summarises the *C*/*I* link analysis for the different reuse pattern sizes and for FFT and GI parameter values. The values presents the percentage of the over-sized legs of distances between the cell sites compared to the amount of all the legs.

Table 4. The *C*/*I* link analysis for QPSK cases.

	Reuse pattern size (*K*)							
FFT,GI	***3***	***4***	***7***	***9***	***12***	***16***	***19***	***21***
8K, 1/4	0	0	0	0	0	0	0	0.5
4K, 1/4	0	0	0	11.1	24.2	36.7	42.1	47.1
2K, 1/4	0	16.7	42.9	55.6	65.2	72.5	75.4	78.1
8K, 1/8	0	0	0	11.1	24.2	36.7	42.1	47.1
4K, 1/8	0	16.7	42.9	55.6	65.2	72.5	75.4	78.1
2K, 1/8	100	100	100	100	100	100	100	100
8K, 1/16	0	16.7	42.9	55.6	65.2	72.5	75.4	78.1
4K, 1/16	100	100	100	100	100	100	100	100
2K, 1/16	100	100	100	100	100	100	100	100
8K, 1/32	100	100	100	100	100	100	100	100
4K, 1/32	100	100	100	100	100	100	100	100
2K, 1/32	100	100	100	100	100	100	100	100

The *C*/*I* link analysis shows that in case of large network (21 cells in the SFN area), the only reasonable parameter set for the QPSK modulation seems to be FFT=8K and GI=1/4. This is due to the fact that QPSK provides with the largest cell sizes (with the investigated parameter set the *r* is 7.5 km). The cell size of the investigated 16-QAM case is smaller (*r*=5.0 km) which provides the use of the parameter set of (FFT = 8K, GI = 1/4), (FFT = 4K, GI = 1/4) and (FFT = 8K, GI = 1/8). The interference distance $r_{interference}$ = 13.5 km is the same in all the cases as the interference affects until it reaches the reference level (the sum of noise floor and terminal noise figure).

The *C*/*I* link investigation gives thus a rough idea about the most feasible parameter settings. In order to obtain the information about the complete performance of DVB-H, the combination of the SFN gain and SER level should be investigated as shown next.

Table 5. The C/I link analysis for 16-QAM cases.

	Reuse pattern size (*K*)							
FFT,GI	***3***	***4***	***7***	***9***	***12***	***16***	***19***	***21***
8K, 1/4	0	0	0	0	0	0	0	0
4K, 1/4	0	0	0	0	0	0.8	1.8	5.7
2K, 1/4	0	0	14.3	30.6	42.4	49.1	57.9	61.9
8K, 1/8	0	0	0	0	0	0.8	1.8	5.7
4K, 1/8	0	0	14.3	30.6	42.4	49.1	57.9	61.9
2K, 1/8	100	100	100	100	100	100	100	100
8K, 1/16	0	0	14.3	30.6	42.4	49.1	57.9	61.9
4K, 1/16	100	100	100	100	100	100	100	100
2K, 1/16	100	100	100	100	100	100	100	100
8K, 1/32	100	100	100	100	100	100	100	100
4K, 1/32	100	100	100	100	100	100	100	100
2K, 1/32	100	100	100	100	100	100	100	100

Figures 29 and 30 show examples of two extreme cases of the simulations, i.e. the PDF of non-interfered and completely interfered situation.

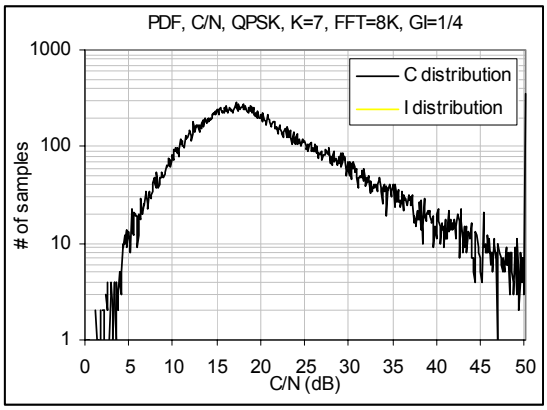

Figure 29. An example of the *C/N* distribution in non-interfered SFN network.

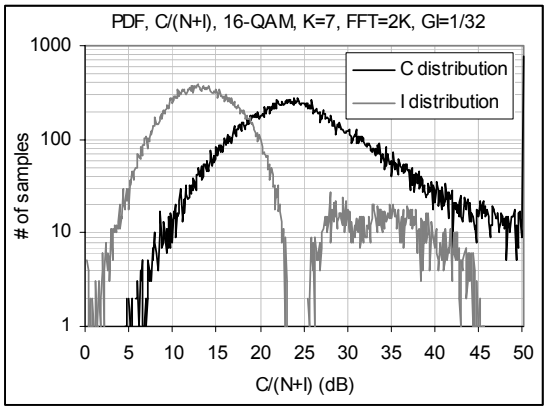

Figure 30. An example of *C/N* and *I/N* in interfered case. This parameter combination does not provide functional service in simulated area.

Figures 29 and 30 show two examples of the PDF, i.e. occurred amount of samples per *C/N* and *C/I* in scale of 0-50 dB, with 0.1 dB resolution.

The PDF gives a visual indication about the general quality of the network. Nevertheless, in order to obtain the exact values of the performance indicators, a cumulative presentation is needed. Figure 31 shows an example of the CDF in the non-interfering QPSK network with the reuse pattern size as a variable. The case shows the *C/N* for the parameter set of QPSK, GI 1/4 and FFT 8K. This mode is the most robust against the interferences as it provides with the longest guard distance.

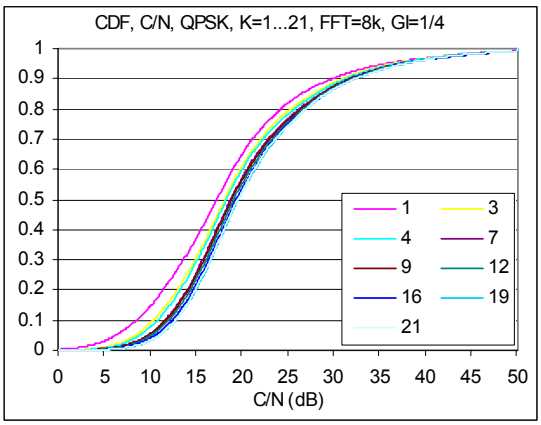

Figure 31. The CDF of C/N in non-interfered network for reuse pattern sizes of 1-21.

Figure 32 shows an amplified view to the critical point, i.e. to the 10% outage probability point.

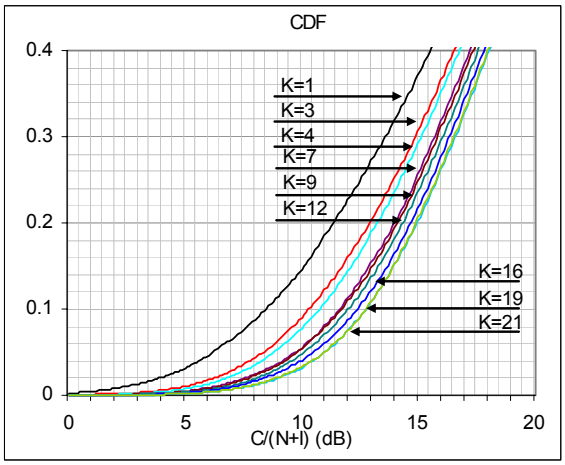

Figure 32. An amplified view of the example of the processed simulation results for QPSK.

As can be seen from Figure 32, the single cell (K=1) results a minimum of 8.5 dB for the 10 % outage probability, i.e. for the area location probability of 90% in the whole cell area which corresponds to the 70% area location probability in the cell edge. The cell is thus correctly dimensioned for the simulations.

In order to find the respective SFN gain level, the comparison with single cell and other reuse pattern sizes can be made in this 10% outage point. The following Figures 33 and 34 shows the respective simulation results for all the symmetrical reuse pattern sizes 1-21 for QPSK and 16-QAM.

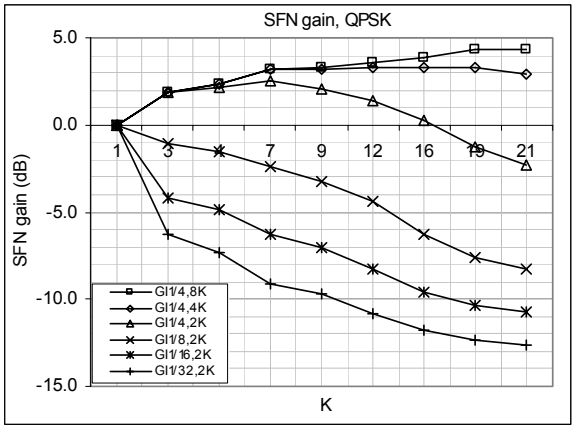

Figure 33. SFN gain levels for QPSK cases, with the reuse pattern sizes of 1-21.

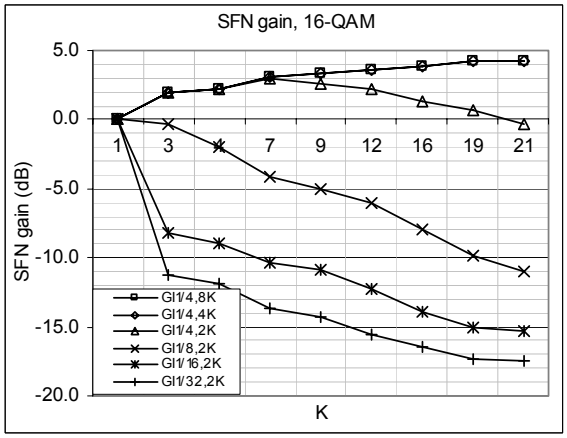

Figure 34. SFN gain levels for 16-QAM cases, with the reuse pattern sizes of 1-21.

The simulation results show the level of SFN gain. The reference case {FFT 8K and GI 1/4} results the maximum gain for the reuse pattern sizes of K=1-21 for both QPSK and 16-QAM and provides a non-interfering network. In addition, the parameter set of {FFT = 4K, GI = 1/4} and {FFT = 8K, GI = 1/8} results a network where SFN errors can be compensated with the SFN gain.

According to the results shown in Figure 33, the QPSK case could provide SFN gain of 3-4 dB in non-interfering network. It is interesting to note that in the interfering cases, also the parameter set of {GI = 1/4, FFT = 4K corresponding FFT = 8K, GI = 1/8} results positive SFN gain even with the interference present for all the reuse pattern cases up to 21. Also the parameter set of {GI = 1/4, FFT = 2K, corresponding FFT = 8K, GI = 1/16 and FFT = 4K, GI = 1/8} provides an adequate quality level until reuse pattern of 16 although the error level (SER) increases.

According to Figure 34, the 16-QAM gives equal SFN gain, resulting about 3-4 dB in non-interfering network. For the {FFT = 4K, GI = 1/4} and the corresponding parameter set of {FFT = 8K, GI = 1/8}, the SFN gain is higher than the SER even with higher reuse pattern sizes compared to QPSK, because the 16-QAM cell size is smaller.

As can be seen from Figures 33-34 and from the C/I link analysis of Tables 4-5, the rest of the cases are practically useless with the selected parameter set.

6. Methodology for the simulations: third variation (urban SFN network)

The dense and urban area of Mexico City was used as a basis for the next simulations as described in [11] by applying suitable propagation prediction models (Okumura-Hata and ITU-R P.1546-3).

6.1. Simulation environment

The city is located on relatively flat ground level with high mountains surrounding the centre area. The height of the planned DVB-H site antennas was 60, 190, 30, 20, 20, 30 and 60 meters from the tower base, respectively for the sites 1-7. The site number 7 represents the mountain installation with the tower base located 800 meters above the average ground level which results the effective antenna height of 860 meters compared to the city centre level. Site number 4 is also situated in relatively high level, but in this case, the surrounding area of the site limits its coverage area. The rest of the sites are located in the base level of Mexico City centre.

As the cell radius of the investigated sites is clearly smaller than 20 km, the Okumura-Hata [3] is suitable for the path loss prediction for all the other sites except for the mountain site number 7. Figure 38 shows the principle of the geographical profile of this site, varying the horizontal angle from the site to the centre

by 10 degree steps. As the profile shows, there are smaller mountains found in front of the site.

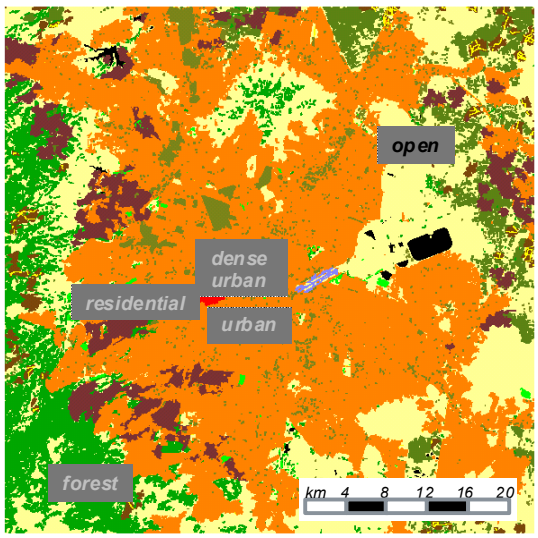

Figure 35. The clutter type of the investigated area.

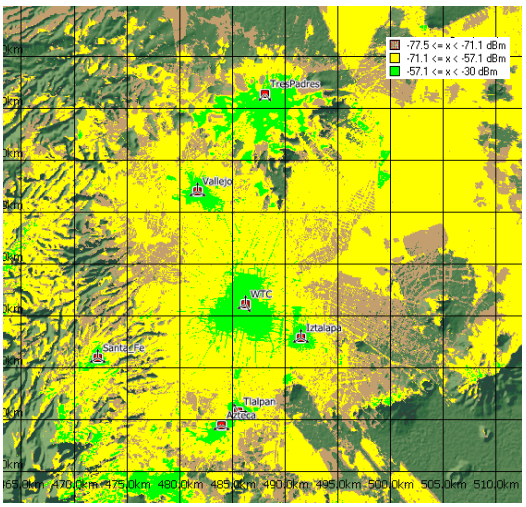

Figure 36. The predicted coverage area of the investigated network as analyzed with a separate radio network planning tool.

Figure 37 presents the location of the selected sites, and the Table 6 shows the site parameters.

For the site number 7, ITU-R P.1546 (version 3) [7] model was applied by using the antenna height of 860 meters and frequency of 680 MHz.

The calculation of the path loss for the site number 7 was done in practice by interpolating the correct ITU-R P.1546 curve for 860 meter antenna height (via 600 and 1200 meter heights) and for 680 MHz frequency (via 600 and 2000 MHz). Figure 39 shows the resulting curve after the iterations.

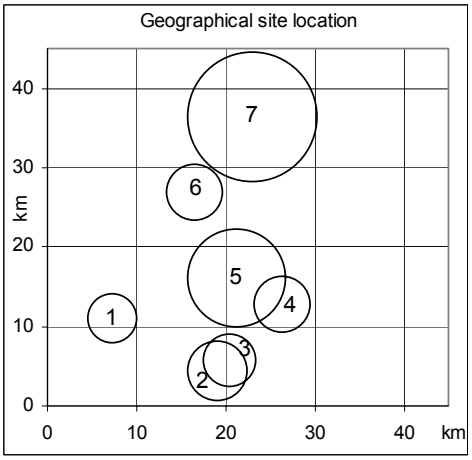

Figure 37. The site locations and informative relative site sizes of the simulator.

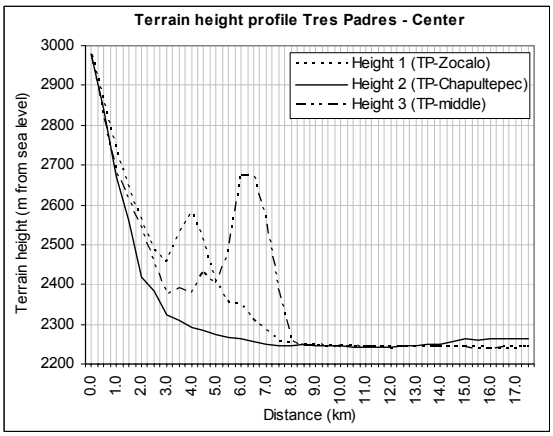

Figure 38. The profile of the mountain site 7.

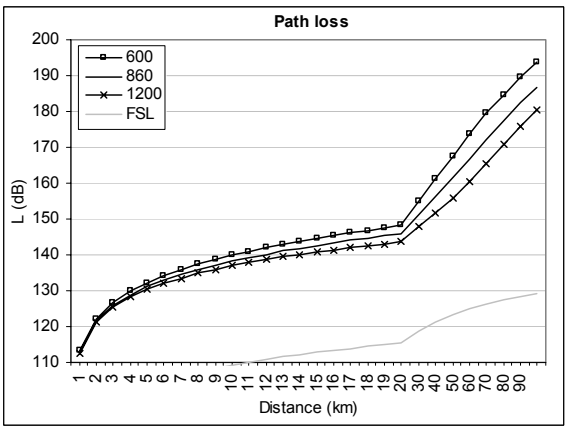

Figure 39. The estimated path loss *L* for the mountain site. FSL is free space loss reference.

Next, a trend line was created in order to present the tabulated values with a closed formula and to ease the simulations. For this specific case, there was one formula created for the path loss in distances of 1-20 km (L_{20}) and another one for the distances of 20-100 km (L_{100}), d being the distance (km):

$$L_{20} = 10.659 \ln(d) + 113.84 \quad (18)$$

$$L_{100} = 0.5124d + 135.55 \quad (19)$$

In order to estimate the error between the trend lines and the original ITU-model, Figure 40 was produced. In the functional area of the mountain site, the maximum error is < 0.5 dB.

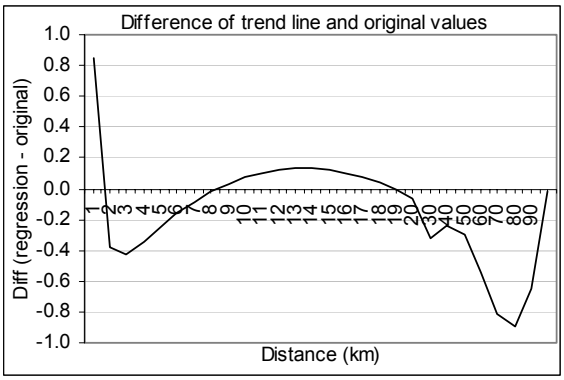

Figure 40. The estimated error margin for the trend lines used for the mountain site path loss calculation.

The link budget of the simulator takes into account separately the radiating power levels and antenna heights of each site as seen in Table 6.

Table 6. The site parameters.

Site	*Coord., km*		*EIRP*		*Radius, km*	
nr	x	y	dBm	W	QPSK	16-QAM
1	7.2	11.0	70.5	11258	4.1	2.8
2	19.0	4.4	69.3	8481	5.6	3.8
3	20.5	5.8	69.3	8481	4.6	3.2
4	26.4	12.7	69.5	8860	5.0	3.4
5	21.2	16.1	71.3	13411	15.5	9.8
6	16.6	27.0	69.3	8481	5.0	3.4
7	23.0	36.4	71.1	12837	26.3	15.8

During the simulations, the receiver was placed randomly in the investigated area (45km × 45km = 2025 km^2) according to the snap-shot principle and uniform geographical distribution. In each simulation round, the separate sum of the carrier per noise and the interference per noise was calculated by converting the received power levels into absolute powers. The result gives thus information about the balance of SFN gain and SFN interference levels. Tables of geographical coordinates with the respective sum of carriers and interferences were created by repeating the simulations 60,000 times. Also carrier and interference level distribution tables were created with a scale of -50 … +50 dB.

The long-term as well as Rayleigh fading was taken into account in the simulations by using respective distribution tables independently for each simulation round. A value of 5.5 dB was used for the standard deviation. The area location probability in the cell edge of 90% was selected for the quality criteria, producing about 7 dB shadowing margin for the long-term fading. Terminal antenna gain of -7.3 dBi was used in the calculations according to the principles indicated in [3]. Terminal noise figure of 5 dB was taken into account. Both Code Rate and MPE-FEC Rate were set to 1/2.

6.2. Simulation results

The usable coverage area was investigated by post-processing the simulation results. The simulations were carried out by using QPSK and 16-QAM modulations, CR ½, MPE-FEC ½ and all the possible variations of FFT and GI.

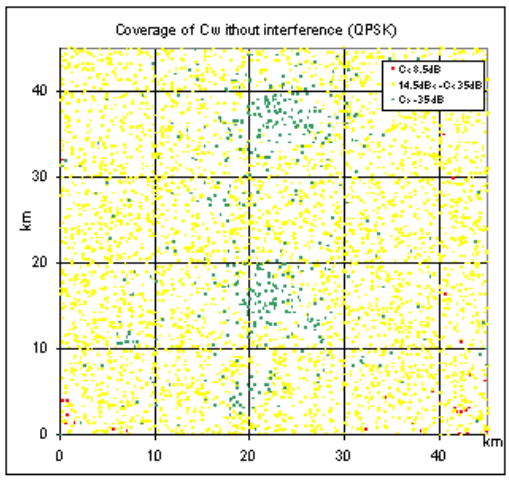

Figure 41. Example of the non-interfered network with the parameter setting of QPSK, GI=1/4 and FFT = 8k.

As expected, the parameter set of {QPSK, FFT 8k, GI 1/4} produces the largest coverage area practically without interferences (Figure 41). The results of this

case can be considered thus as a reference for the interference point of view.

When the GI and FFT values are altered, the level of interference varies respectively. The results show that in addition to the parameter set of {FFT 8k, GI 1/4}, also {FFT 8k, GI 1/8}, {FFT 4k, GI 1/4} produces useful coverage areas, i.e. the balance of the SFN gain and SFN interferences seem to be in acceptable levels, whilst the other parameter settings produces highly interfered network.

The 16-QAM produces smaller coverage areas compared to the QPSK as the basic requirement for the $C / (N + I)$ of 16-QAM is 14.5 dB instead of the 8.5 of QPSK.

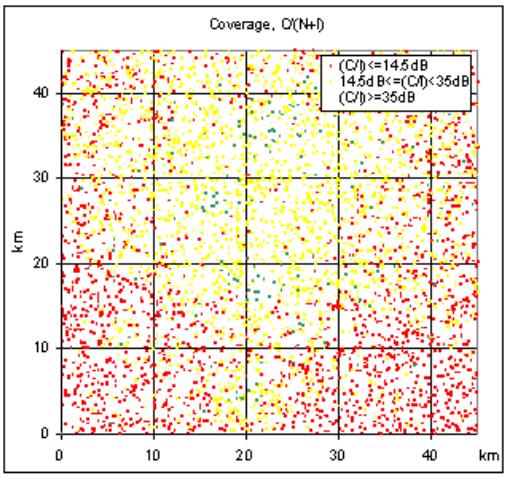

Figure 42. Comparative example of the simulation results for the parameter set of 16-QAM, FFT 8k and GI 1/16.

As can be observed from the previous analysis and Figure 42, the SFN interferences tend to cumulate to the outer boundaries of the planned coverage area.

For the QPSK with FFT 8k and GI ¼, the area is practically free of interferences, i.e. the $C / (N + I)$ is > 8.5 dB in every simulated location. The dark colour in the middle shows the site locations with the $C / (N + I)$ greater than 35 dB.

By observing the 90% probability in the cell edge (about 95% in the cell area), i.e., 5 % outage probability of Figures 43-44, the mode {FFT 8k, GI 1/4} provides a minimum of about 7 dB and the set of {FFT 8k, GI 1/8} and {FFT 4k, GI 1/4} provides the same performance in the whole investigated area. This similarity is due to the D_{sfn} limit, which is complied totally in both of the cases as the sites are grouped inside about 30 km diameter. It is worth noting that the values are calculated over the whole map of 45km × 45km.

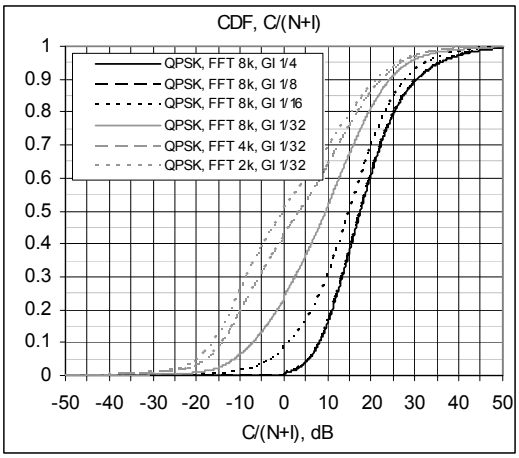

Figure 43. The cumulative $C/(N+I)$ distribution of different modes for QPSK.

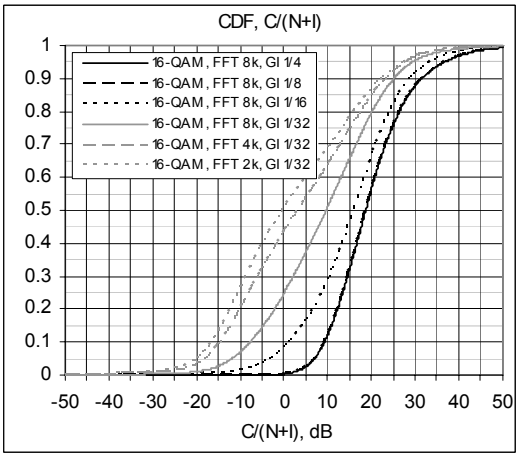

Figure 44. The cumulative $C/(N+I)$ distribution of different modes for 16-QAM.

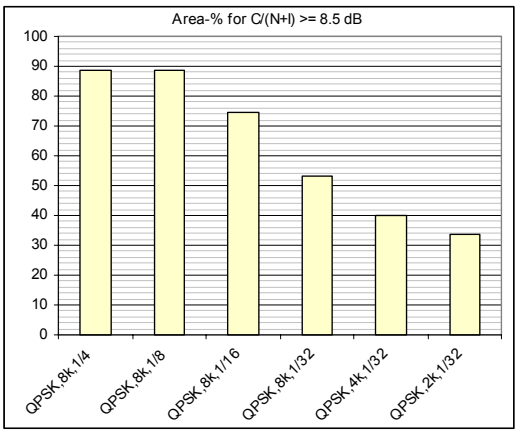

Figure 45. The functional area percentage for QPSK modes compared to the total area.

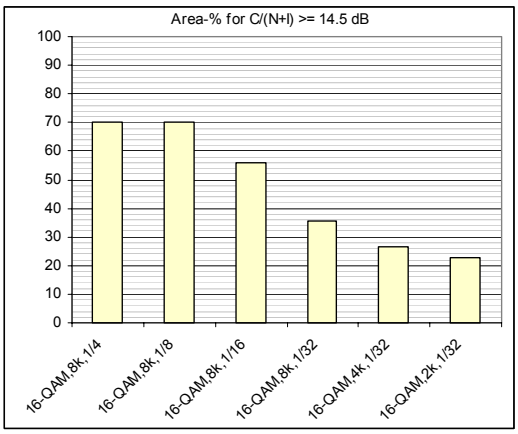

Figure 46. The functional area percentage for 16-QAM modes compared to the total simulated area.

It seems that the QPSK mode would provide a good performance in the investigated area when using the non-interfering {FFT 8k, GI 1/4} parameters, whilst 16-QAM gives smaller yet non-interfered coverage area. The advantage of the latter case is the double radio channel capacity compared to the QPSK with greater coverage area. The parameter set of {FFT 8k, GI 1/8} and {FFT 4k, GI 1/4} looks also useful, providing the possibility to either rise the maximum velocity of the terminal (FFT 4k), or give more capacity (GI 1/8). As for the rest of the parameter settings, the optimal balance can not be achieved due to the raised interference levels.

The SFN gain of the investigated network could be observed more specifically by switching on and off the individual sites, by carrying out the $C / (N + I)$ simulations and by noting the differences in the cumulative density function. This is not, though, accurate method unless the simulations are limited inside the maximum calculated cell radius of each site. The network layout used in this case is highly irregular and does not contain too much overlapping areas compared to the total area of 45 km × 45 km, so the separate SFN gain investigation was not carried out. On the other hand, the presented results already include the total sum of the SFN gain and interference.

It can be estimated though that especially with the QPSK modes that provides with the largest coverage areas, the mountain site does have an effect within the overlapping areas of the nearest cells. According to the simulations presented in Figure 33, this case could provide an SFN gain of about 1 dB in such areas. Similarly, if there is spot with three overlapping cells in the middle of the area (i.e. in the area without interferences), the SFN gain could be around 2 dB according to the simulations presented in the chapter showing the balance of the SFN gain and SFN interferences. The results presented in [9] support this observation.

7. Conclusion

The presented simulation method provides both geographical and cumulative distribution of the SFN gain and interference levels. The method takes into account the balancing of the coverage and capacity as well as the optimal level of SFN gain and the interference level in case the over-sized SFN is used. It can be applied for the theoretical, e.g. hexagonal cell layouts, as well as for the practical environments, taking into account the radio propagation modelling for different sites.

The method can thus be used in the detailed optimization of the DVB-H networks. The principle of the simulator is relatively straightforward and the method can be applied by using various different programming languages. In these investigations, a standard Pascal was used for programming the core simulator.

The SFN gain results are in align with the practical results of e.g. [4] and [5] for the low number site. For the high number of the sites, no reference results were found due to the practical challenges in setting up the test cases. Nevertheless, estimating the theoretical limits by applying the formula 5, the results are in logical range. The SFN interference level results behave also logically and are in align with e.g. [10].

The results show that the radio parameter selection is essential in the detailed planning of the DVB-H network. As the graphical presentation of the results indicate, the effect of the parameter value selection on the interference level and thus on the quality of service can be drastic, which should be taken into account in the detailed planning of DVB-H SFN.

Especially the controlled extension of the SFN limit might be interesting option for the DVB-H operators. The simulation method and related results shows logical behaviour of the SFN error rate when varying the essential radio parameters. The results also show that the optimal setting can be obtained using the respective simulation method by balancing the SFN gain and SFN errors. As expected, the 8K mode is the most robust when extending the SFN whilst 4K limits the maximum site antenna height. 16-QAM provides suitable performance for the extension, but according to the results, even QPSK which provides larger coverage areas is not useless in SFN extension when selecting the parameters correctly.

8. References

[1] Jyrki T.J. Penttinen. The SFN gain in non-interfered and interfered DVB-H networks. The Fourth International Conference on Wireless and Mobile Communications 2008, IARIA, Published by the IEEE CS Press. 6p.

[2] DVB-H Implementation Guidelines. Draft TR 102 377 V1.2.2 (2006-03). European Broadcasting Union. 108 p.

[3] Masaharu Hata. Empirical Formula for Propagation Loss in Land Mobile Radio Services. IEEE Transactions on Vehicular Technology, Vol. VT-29, No. 3, August 1980. 9 p.

[4] Maite Aparicio (Editor). Wing TV. Services to Wireless, Integrated, Nomadic, GPRS-UMTS&TV handheld terminals. D8 – Wing TV Country field trial report. Project report, November 2006. 258 p.

[5] David Plets. New Method to Determine the SFN Gain of a DVB-H Network with Multiple Transmitters. 58th Annual IEEE Broadcast Symposium, 15-17 October 2008, Alexandria, VA, USA. 6 p.

[6] Jyrki T.J. Penttinen. The Simulation of the Interference Levels in Extended DVB-H SFN Areas. The Fourth International Conference on Wireless and Mobile Communications 2008, IARIA, Published by the IEEE CS Press. 6 p.

[7] Recommendation ITU-R P.1546-3. Method for point-to-area predictions for terrestrial services in the frequency range 30 MHz to 3000 MHz. 2007. 57 p.

[8] Gerard Faria, Jukka A. Henriksson, Erik Stare, Pekka Talmola. DVB-H: Digital Broadcast Services to Handheld Devices. IEEE 2006. 16 p.

[9] William C.Y. Lee. Elements of Cellular Mobile Radio System. IEEE Transactions on Vehicular Technology, Vol. VT-35, No. 2, May 1986. pp. 48-56.

[10] Airi Silvennoinen. DVB-H –lähetysverkon optimointi Suomen olosuhteissa (DVB-H Network Optimization under Finnish Conditions). Master's Thesis, Helsinki University of Technology, 15.5.2006. 111 p.

[11] Jyrki T.J. Penttinen. DVB-H Performance Simulations in Dense Urban Area. The Third International Conference on Digital Society, ICDS 2009, IARIA, Published by the IEEE CS Press. 6 p.

[12] Minseok Jeong. Comparison Between Path-Loss Prediction Models for Wireless Telecommunication System Design. IEEE, 2001. 4 p.

Biography

Mr. Jyrki T.J. Penttinen has worked in telecommunications area since 1994, for Telecom Finland and it's successors until 2004, and after that, for Nokia and Nokia Siemens Networks. He has carried out various international tasks, e.g. as a System Expert and Senior Network Architect in Finland, R&D Manager in Spain and Technical Manager in Mexico and USA. He currently holds a Senior Solutions Architect position in Madrid, Spain. His main activities have been related to mobile and DVB-H network design and optimization.

Mr. Penttinen obtained M.Sc. (E.E.) and Licentiate of Technology (E.E.) degrees from Helsinki University of Technology (TKK) in 1994 and 1999, respectively. He has organized actively telecom courses and lectures. In addition, he has published various technical books and articles since 1996.